Advance Research in Textile Engineering

Open Access

Austin Publishing Group

Research Article

Prediction of Micro Mechanical Behavior of 3D Orthogonal Woven Composite Structure Produced from Different Yarn Cross-sections

Sameer Kumar Behera[1]; Soumya Chowdhury[2]; Harsh Chauhan[2]; Behera BK[2*]

[1]School of Interdisciplinary Research, Indian institute of Technology Delhi, India

[2]Department of Textile & Fiber Engineering, Indian Institute of Technology Delhi, India

***Corresponding author:** **Behera BK**

Department of Textile & Fiber Engineering, Indian Institute of Technology Delhi, India.

Email: behera@textile.iitd.ac.in

Received: January 18, 2024

Accepted: March 08, 2024

Published: April 15, 2024

Abstract

This paper focuses on investigating the influence of yarn cross-sectional geometry on the tensile behaviour of 3D woven fabric-reinforced composites. As the demand for advanced engineering applications increases, 3D woven composites have become a popular choice due to their superior mechanical properties compared to traditional materials. However, it is crucial to understand the micromechanical behaviour of these composites in a specific woven construction to predict their mechanical properties accurately. To achieve this objective, the study utilized an analytical model to analyse the tensile behaviour of 3D woven fabric-reinforced composites with two different yarn cross-sections, elliptical and lenticular. The cross-sectional geometry of the yarns is a critical factor that can influence the thickness of the 3D woven preforms, ultimately affecting the mechanical behaviour of the composite materials. MATLAB coding was used to establish a good correlation with the established analytical models for both types of yarn cross-sections. Furthermore, computational models were developed using the ANSYS platform to compare the tensile behaviour of the two yarn cross-sections. The experimental tests were carried out according to ASTM standards to validate the findings and ensure the accuracy and reliability of the numerical results. The results revealed that the elliptical cross-sectional model exhibited better agreement with both the computational and experimental outcomes when compared to the lenticular model. This suggests that the yarn cross-sectional geometry, particularly the use of elliptical cross-sections, plays a significant role in determining the mechanical behaviour of 3D woven fabric-reinforced composites. These findings provide valuable insights for researchers and engineers in selecting appropriate yarn cross-sectional geometries to predict the mechanical properties of 3D woven composites accurately.

Keywords: Microstructural analysis; Fabrics/textiles Micro-mechanical; Resin Transfer Moulding (RTM); Numerical analysis

Introduction

In recent times, advanced engineering industries such as automobiles, aerospace, and green energy have shown a growing interest in 3D woven composite materials due to their superior advantages over traditional metals and alloys. Fibre-reinforced composites offer numerous benefits such as high modulus and strength, lightweight, corrosion resistance, and excellent formability compared to conventional materials like aluminium alloys However, laminate composites, despite having greater mechanical qualities than typical alloys, are susceptible to impact damage and delamination. Although laminate composites offer outstanding mechanical attributes compared to classical equivalents, they are not ideal due to their high production costs, quick delamination, and impact damage. Therefore, three-dimensional weaving presents a potential solution to this problem by producing an integrally connected 3D network of fibres with near-net shape dry preforms and substantial thickness by introducing through-thickness yarn. The enhanced structural stability of 3D woven composites has generated significant interest in the industry. Overall, 3D woven composites have two distinct advantages: all fibers are contained within a single preform, and through-thickness yarn, also known as binder yarn, is present [5-7]. In addition, 3D woven fabrics offer several ad-

Citation: Behera SK, Chowdhury S, Chauhan H, Behera BK. Prediction of Micro Mechanical Behavior of 3D Orthogonal Woven Composite Structure Produced from Different Yarn Cross-sections. Adv Res Text Eng. 2024; 9(2): 1099.

vantages over conventional 2D fabrics, such as the ability to use distinct fibers in different directions, flexibility in controlling the Fibre-Volume-Fraction (FVF), and the arrangement of yarns to meet specific objectives. They also have higher impact tolerance, lower manufacturing costs, and improved repeatability compared to their 2D counterparts [8]. Analytical and computational modelling can predict the mechanical properties of composite materials, which can guide optimization for selecting appropriate composite structures for suitable applications. Otherwise, the experimental method can be expensive and time-consuming to determine mechanical characterization for use in a particular application. However, the complex nature of 3D woven fabrics brings a lot of challenges in predicting the mechanical properties of 3D woven composites due to their anisotropy and the enormous number of mechanical variables [2] Composites are considered heterogeneous materials since they are made up of two unique elements, matrix and reinforcement (3D fabric in this case), each with distinct physical and mechanical properties. In terms of microstructural metrics such as FVF, yarn cross-section, and yarn orientation, a heterogeneous material is generally anisotropic. Because of the heterogeneity of the composite, it has become necessary to analyse the composite at the constituent level. The main benefit of assessing micromechanics is that it may predict virtual testing of a composite sample, which helps to lower the cost of the trials. A model to predict the stiffness matrix of the composite was proposed by A. Mahmood et al. [9] in which it is shown that the elastic constant of the composite not only depends on the elastic constants of its constituents but also depends upon their respective fraction of volume. And if the cross-sections of the yarns are changed, the fibre volume fraction (FVF) in the tow considered will change according to the below equation (42) [10]. The aforementioned equations make it evident that the mechanical constants will vary with the varied cross-section of the yarn. As a result, it is critical to understand that by taking into account the cross-section, the Model predicts elastic constant values that are close to experimentally found values.AR Labanieh et al. [11] used the finite element methodology to investigate the impact of the binder tows configuration on the through-the-thickness components of stresses in their proposed model. SZH Shah et al. [12] proposed a two-step method (micro-meso and meso-macro homogenization) to predict the elastic modulus of three-dimensional fibre-reinforced composites. According to A. Mahmood et al.'s [13] micromechanical model, tow geometric parameters, including cross-sectional shape, path, and position within the textile structures, as well as preform geometric parameters such as volume proportions of individual fibres, overall fibre volume fraction, and preform thickness, are critical for predicting the mechanical properties of composites. Nehme S et al. [14] used an analytical model to predict the mechanical behaviour of interlock woven composites by modelling the yarns' geometry using a sinusoidal function and homogenizing at the macro-level based on both iso-strain and iso-stress assumptions. VR Jayan et al. [15] used mathematical coding, modelling, and simulation with Solid works and Ansys to predict the interior geometry and tensile behaviour of 3D woven solid structures. [16] have presented different models and investigations. Cox et al. [17] investigated microstructural characteristics and failure processes in 3D woven composites. Callus et al. [18] investigated the tensile failure mechanisms of three distinct 3D weaving structures fabricated from glass-reinforced polymer composites to complement Cox et al.'s work.

The researchers investigated the influence of increasing tensile loads on woven structures and identified the point of microstructural deterioration. However, the impact of fiber cross-sectional geometry in fabric preforms under tensile load remains unexplored. The mechanical properties of composites depend not only on the original characteristics of the constituents but also on geometric factors such as fiber orientation, yarn architecture, fiber cross-section, and fiber volume fraction.

As of now, there is no literature available that specifically addresses the comparison between two different fiber cross-sectional geometries. Changing the yarn's cross-section not only affects the volume percentage of fibers in the dry preform but also influences the overall thickness of the composite. Therefore, gaining a comprehensive understanding and obtaining experimental evidence are crucial for determining critical fiber cross-sectional values in preforms. This information is essential for researchers to accurately predict mechanical properties through simulation.

In this study, considered two different yarn cross-sections, elliptical and lenticular, using an established analytical model. The primary objective was to evaluate the effect of yarn cross-section (microscale geometry) on the tensile behaviour of 3D woven fabric-reinforced composites through computational methods using the ANSYS platform based on the aforementioned analytical model [10]. The computational models were performed, taking the yarn cross-sectional geometry as the primary factor. This investigation aimed to assist researchers in organizing analytical and computational models for predicting mechanical properties, particularly when the micro-scale geometry of reinforcement plays a direct role in determining the thickness of performs. The computational results were validated through experiment data, aiming to find the close proximity between the established analytical and developed computational models with the presented experimental results.

Material and Methods

Materials

In this experiment, E-glass tow of 600 tex was used to manufacture 3D orthogonal woven preform as reinforcement and Epoxy Resin (Lapox ARL-125) as matrix parts. E-glass tow and resin Lapox ARL-125 and its equivalent hardener Lapox AH-365 were supplied by Owen's corning and Atul India pvt. Ltd, respectively. The properties of glass fiber and epoxy resin are given in table no. 1 and 2 respectively.

Table 1: Properties of glass fiber.

Properties	Value
Density	2.54g/cc
Modulus of Elasticity	76 Gpa
Tensile Strength	3.2 Gpa
Breaking elongation	2.53 %
Poisson's Ratio (PR)	0.21
Modulus of Shear	31 Gpa

Table 2: Properties of Epoxy resin.

Properties	Value
Tensile Strength	60-70 Mpa
Modulus of Elasticity	2.8-3.4 Gpa
Modulus of Shear	3.0-3.6 Gpa
Poisson's Ratio (PR)	0.29-0.35
Elongation at Break	4-7 %

Table 3: Comparison between experimental and analytical results.

Property	Experimental	Analytical		
	Elliptical	Elliptical	Error (%)	Lenticular
Elastic Modulus in X-Direction (GPa)	16.65	18.87	11.76	15.47
Elastic Modulus in Y-Direction (GPa)	21.72	19.40	-11.95	16.03

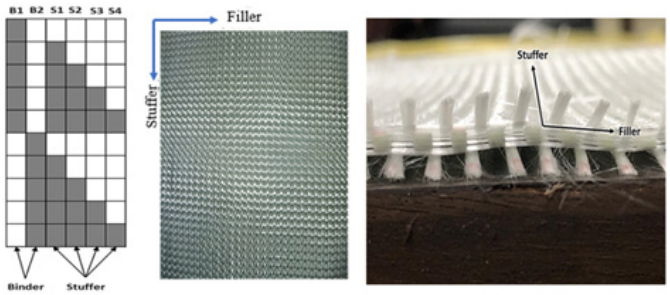

Figure 1: Weave Pattern and 3D orthogonal Fabric prepared (Top View and Cross-sectional View).

3D Orthogonal Fabric Preparation

3D orthogonal plain 1X1 woven structure was manufactured at Focus Incubation Centre: 3D waving and Structural Composites at IIT Delhi by using a customized 3D weaving loom. A 600 tex E-glass fiber is used in all the three directions, i.e., stuffer (X), filler (Y), and binder (Z). The top and cross-sectional view of the fabric is shown in Figure 1

The fabric has the following specifications:

- **Weave**: 1x1 Plain Weave
- **Glass Fiber**: 600 tex
- **Fabric Width**: 16 inches
- **Fabric Structure**: 4 Stuffer Layer Structure
- **EPI (ends per inch)**: 30 (20S+10B)
- **PPI (picks per inch)**: 12
- **GSM**: 2066.6667 ±100 (approx.)
- **Total No. of Warp Ends**: 480 (320 Stuffer ends + 160 Binder ends)
- **Reed**: 10 dpi (dent per inch)

Preparation of Composite

The composite is prepared by using the Vacuum Assisted Resin Transfer Moulding (VARTM) method. In this process, manufactured 3D orthogonal woven preform is used as reinforcement and epoxy resin as matrix. To control preferred Fibre Volume Fraction throughout the composite plate VARTM process was taken into consideration for transferring preform into composites. In VARTM process, a vacuum pressure was created by using a vacuum pump and covering the glass bed by 70-micron vacuum film bag. In this process, the fabric was in rested position, and then the resin was impregnated from one side while the vacuum pump keeps maintain negative pressure bar for the resin to wet the preform completely by flowing to the other side. The resin flowed through the fabric as shown in Figure 2(a) and after completing the process, it was left for 24 hours for curing. At the end, a semi-transparent plate was prepared as shown in Figure 2 (b).

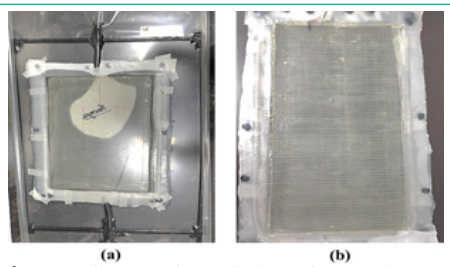

Figure 2: (a) Resin Flowing Through the Fabric in the Vacuum Bag, **(b)** The composite Plate Prepared.

The composite plate made has given parameters:

- Length of composite plate: 40 cm
- Width of composite plate: 30 cm
- Weight of the fabric taken: 248 gm
- Weight of the resin taken: 300 gm (resin) + 96 gm (hardener)
- Time given to composite for curing: 48 hrs
- Fiber Volume Fraction: 48.9%

Testing of the Composite

Testing of the composite material was conducted in accordance with the ASTM D3039 standard using a Zwick/Roell Z250 Universal Testing Machine. The composite plate was cut into specimens along the warp and weft directions, following the standardized dimensions of 25 cm x 2.5 cm. A gauge length of 15 cm was maintained by gripping 5 cm of the specimen length from both sides using the machine jaws, as illustrated in Figure 3(a). The samples were clamped in the Zwick/Roell testing machine, with the upper jaw moving at a speed of 2 mm/min while the lower jaw remained fixed. The clamps were adjusted to apply a pressure of 15-18 Bar, which was determined using the hit and trial method. Maintaining optimum pressure during the testing process is essential to ensure accurate results. Inadequate pressure applied to the sample may lead to slipping of the specimen from the jaws, resulting in erroneous results. On the other hand, excessive pressure could cause unwanted cracks in the gripped portion of the composite specimen, leading to incorrect outcomes. Therefore, it is important to carefully calibrate the clamps on the machine to apply the appropriate pressure range, as determined by the trial-and-error method. By ensuring proper pressure, the accuracy and reliability of the test results can be improved. The tested sample in both warp and weft directions are shown in Figure 3(b) and 3(c).

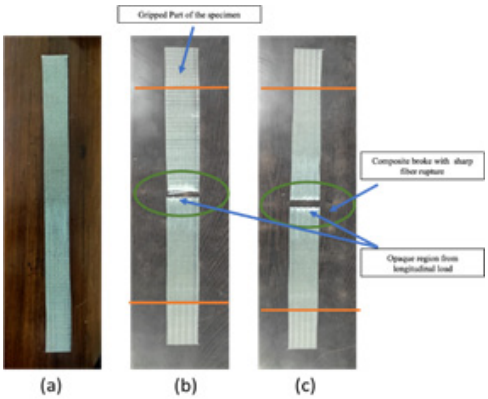

Figure 3: (a) Untested Sample Strip, **(b)** Tested Warp Way Sample Strip, **(c)** Tested Weft Way Sample Strip.

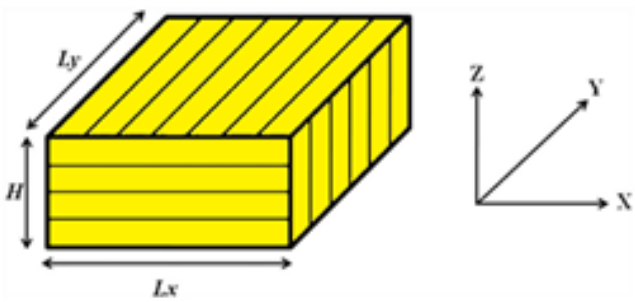

Figure 4: Dimensions of a Unit Cell.

Modelling Approach

Analytical Modelling

The geometrical model of a 3D orthogonal woven structure utilized in this research was originally proposed by S. Buchanan et al. [19] and later modified by B.P. Dash et al. [10,15,16] Additionally, a model proposed by A. Mahmood et al. [20] was incorporated to predict the tensile behaviour of the composite material. MATLAB was used to process the equations of these models. To determine the geometry of the composite unit cell, the volume of the three yarns was calculated in three mutually perpendicular directions. This calculation allowed for the determination of the cross-sectional shapes of the yarns and the aspect ratio of each tow, as per the expressions previously derived by Dash et al [21].

The thickness of individual tows can be determined by equations (1) [21]

$$h_i = 2\sqrt{\frac{\mu_i}{\rho AR P_f \pi}} \quad (i = s, f, b)\{for\ elliptical\} \quad (1)$$

Where μ: Linear density of tow (kg/m), ρf: Density of fibre (g/cc), AR: Aspect ratio of tows, P_f: Tow-packing factor, ρ Density of individual tows

Because the tow filaments are elliptical, they could not be fully packed together without gaps; hence a tow-packing factor was used.

$P_f = \pi/4$ (for rectangular packing array)

The entire thickness of the Lenticular unit cell can be computed using Equation (2) [21].

$$h_i = \sqrt{\frac{2*\mu_i}{\rho AR P_f}} \quad (i = s, f, b)\{for\ lenticular\} \quad (2)$$

The thickness of the unit cell of 3D fabric can be calculated by using equation (3) [21]

$$H = n_s * h_s + n_f * h_f + 2 * h_b \quad (3)$$

Where, h_s, h_f, h_b Individual thickness of stuffer, filler and binder tows(m),

n_s, n_f, n_b Total numbers of stuffers, filler and binder layers in unit cell

The individual tow length is determined by equations (4)-(6) [21].

$$l_s = \frac{n_f^{uc}}{\lambda_f} \quad (4)$$

$$l_f = \frac{n_s^{uc}}{\lambda_s} \quad (5)$$

$$l_b = n^{uc}{}_f(h_f AR_f) + 2H \quad (6)$$

Where, l_s, l_f, l_b The individual tow length (stuffer, filler and binder),λ_s, λ_f, λ_b Total number of individual yarns (stuffers, filler and binder)/m in perpendicular direction to tow direction, $n^{uc}{}_f$ Number of filler yarns along stuffer direction in a unit cell.

The Below Equation 7 is calculate the total length of individual warp, filler and binder tows [21]

$$L_i = l_i n_i n_i^{uc} \quad (7)$$

Where i = s, f, b (stuffers, filler and binder)

The component of binder tow in z-direction is [21]

$$Z_{TL} = n_b^{uc} 2H \quad (8)$$

The Below equation (9) can calculate the Cross-Sectional area of each tow [21]

$$A_i = \frac{\mu_i}{\rho P_f} \quad (9)$$

Total tow volume can be given by [21].

$$V_i = l_i A_i \quad (10)$$

The volume of fibers in x direction is sum of the fiber volume fraction of warp yarn and the horizontal component of binder yarn, and only the vertical component of binder yarn participates in the fiber volume fraction in z-direction. Total volume of fiber calculates by equation (11)-(13) [21].

$$X_{TV} = V_s + (L_b - Z_{TL})A_b \quad (11)$$

$$Y_{TV} = V_f \quad (12)$$

$$Z_{TV} = Z_{TL} A_b \quad (13)$$

Where, X_{TV}, Y_{TV}, Z_{TV} are total volume of fibers parallel to the X, Y and Z-direction, V_s, V_f, V_b are total volume of stuffer, filler and binder tows in the unit cell, l_s, l_f, l_b are the individual tow length (stuffer, filler and binder)

The unit cell mass is determined by equation (14), integrating all the linear masses [21].

$$M^{uc} = \sum L_I \mu_I \quad (14)$$

The equation 15 may determine areal density

$$S^{uc} = \frac{M^{uc}}{L_x L_y} \quad (15)$$

Where L_x, L_y are unit cell length in X & Y direction shown in figure 4, M_{uc} is unit cell mass The overall FVF of the unit cell can be determined as the given equation (16) [21].

$$FVF_{uc} = \frac{S^{uc}}{\rho H} \quad (16)$$

The volume fraction of each type (warp, filler & binder) of yarn can be given by the following equations 17:

$$V_{fi} = \frac{V_i}{V_s + V_f + V_b} 100 \ldots\ldots\ldots\ldots\ldots\ldots \{i = s, f, b\} \quad (17)$$

The binder tows are oriented in both x and z-direction; hence its configuration is also considered while calculating the FVF in a particular direction and it can be calculated by given equations:

$$V_{fi} = \frac{i_{TV}}{X_{TV} + Y_{TV} + Z_{TV}} * 100 \ldots\ldots\ldots\ldots \{i = X, Y, Z\} \quad (18)$$

Volume of RVE:

$$V_{RVE} = L_x * L_y * H \quad (19)$$

Where, H Total thickness of the unit cell

Volume proportion of each type of tows:

$$V_{ip} = \frac{V_i}{V_{RVE}} \quad (20)$$

A. Mahmood et al. develop a simplified analytical model for predicting the stiffness matrix of 3D woven orthogonal composites [20]. In this Model at the RVE level, average volume and iso-strain homogeneous boundary conditions are applied. In this model, the tow is a unidirectional lamina whose nature is transversely isotropic. Chamis micromechanical equations (21)-(26) [22] are used to calculate the elastic constants of transversely isotropic tows with respect to local coordinate system (i.e., 1-2-3).

$$E_{11} = \beta E_{11f} + (1-\beta)E_m \quad (21)$$

$$E_{22} = E_{33} = \frac{E_m}{1-\sqrt{\beta}(1-\frac{E_m}{E_{22f}})} \quad (22)$$

$$G_{12} = G_{13} = \frac{G_m}{1-\sqrt{\beta}(1-\frac{G_m}{G_{12f}})} \quad (23)$$

$$G_{23} = \frac{G_m}{1-\sqrt{\beta}\left(1-\frac{G_m}{G_{23f}}\right)} \quad (24)$$

$$\nu_{12} = \nu_{13} = \beta\nu_{12f} + (1-\beta)\nu_m \quad (25)$$

$$\nu_{12} = \frac{E_{22}}{2G_{23}} - 1 \quad (26)$$

Where,

- $E_{11f}, E_{22f}, G_{12f}$, G_{23f}, ν_{12f} = various elastic constants of the fibers.
- E_m, G_m, ν_m = matrix elastic constants (Gpa)
- β = FVF of the tow. 23-plane = isotropic plane,

The following equations (27-31) [20] are used to compute the stiffness matrix of transversely isotropic tows with respect to the 1-2-3 co-ordinate system.

$$\Delta = 1 - 2\nu_{12}\nu_{21} - \nu_{23}^2 - 2\nu_{12}\nu_{21}\nu_{23} \quad (27)$$

$$Q_{11} = \frac{E_{11}(1-\nu_{23}^2)}{\Delta} \quad (28)$$

$$Q_{12} = \frac{E_{22}(\nu_{12}+\nu_{32}\nu_{12})}{\Delta} \quad (29)$$

$$Q_{22} = \frac{E_{22}(1-\nu_{12}\nu_{21})}{\Delta} \quad (30)$$

$$Q_{23} = \frac{E_{22}(\nu_{32}+\nu_{12}\nu_{21})}{\Delta} \quad (31)$$

$$Q_{44} = G_{23}, \quad Q_{55} = G_{12}, \quad Q_{66} = G_{12}$$

Where,

$$[Q] = \begin{bmatrix} Q11 & Q12 & Q12 & 0 & 0 & 0 \\ Q12 & Q23 & Q23 & 0 & 0 & 0 \\ Q12 & Q23 & Q22 & 0 & 0 & 0 \\ 0 & 0 & 0 & Q44 & 0 & 0 \\ 0 & 0 & 0 & 0 & Q55 & 0 \\ 0 & 0 & 0 & 0 & 0 & Q66 \end{bmatrix} \quad (32)$$

Transformed stiffness matrix for warp and fill sets of tows can be calculated by equation (33) [2].

$$[\bar{Q}_i] = [T_i]^{-1}[Q_i][T_i]^{-T} \quad (33)$$

Where, $[T_i]$ = Transformation matrix of warp and filler tows, $[T_i]^{-T}$= transpose of transformation matrix [2].

$$[T_i] = \begin{bmatrix} m^2 & n^2 & 0 & 0 & 0 & 2mn \\ n^2 & m^2 & 0 & 0 & 0 & -2mn \\ 0 & 0 & 1 & 0 & 0 & 0 \\ 0 & 0 & 0 & m & -n & 0 \\ 0 & 0 & 0 & n & m & 0 \\ -mn & mn & 0 & 0 & 0 & m^2-n^2 \end{bmatrix} \quad (34)$$

Where, m = cosα and n = sinα, {α = 0° (warp tow), α = 90° (fill tow)}.

There is a different transformation matrix for z fiber tows as they are situated in x-z plane. The transformed stiffness matrix of these tows is calculated by equation (35) [20].

$$[\bar{Q}_i] = [T_j]^{-1}[Q_z][T_j]^{-T} \quad (35)$$

Where $[T_j]$ = transformation matrix for z-fibers

$$[T_i] = \begin{bmatrix} p^2 & q^2 & 0 & 0 & 2pq & 0 \\ 0 & 1 & 0 & 0 & 0 & 0 \\ q^2 & p^2 & 1 & 0 & -2pq & 0 \\ 0 & 0 & 0 & p & 0 & -q \\ -pq & pq & 0 & 0 & p^2-q^2 & 0 \\ 0 & 0 & 0 & q & 0 & p \end{bmatrix} \quad (36)$$

where p = cos(β), q = sin(β), β = undulation angle of Z fiber tow,

The matrix is considered an isotropic material. The stiffness matrix of the matrix is calculated by the given equations (37)-(40) [20].

$$[Q_m] = \begin{bmatrix} Q_{11} & Q_{12} & Q_{12} & 0 & 0 & 0 \\ Q_{12} & Q_{11} & Q_{12} & 0 & 0 & 0 \\ Q_{12} & Q_{12} & Q_{11} & 0 & 0 & 0 \\ 0 & 0 & 0 & Q_{44} & 0 & 0 \\ 0 & 0 & 0 & 0 & Q_{55} & 0 \\ 0 & 0 & 0 & 0 & 0 & Q_{66} \end{bmatrix} \quad (37)$$

$$Q_{11} = \frac{(1-\nu_m)E_m}{(1-2\nu_m)(1+\nu_m)} \quad (38)$$

$$Q_{12} = \frac{\nu_m E_m}{(1-2\nu_m)(1+\nu_m)} \quad (39)$$

$$Q_{44} = G_m \quad (40)$$

E_m, ν_m, G_m = elastic constants of matrix, the stiffness matrix of a ply can be calculated with the help of volume averaging method as in the given equation (41) [20].

$$[Q_i]_p = \sum V_{ijk}[\overline{Q_{ijk}}] \quad (41)$$

Where j = layer number and k = type of the material of the

tow. $[\overline{Q_{ijk}}]$ is the stiffness matrix of a single tow elements.

The contribution of stiffness of each component is calculated with the help of volume averaging method and the stiffness of the representative volume element is calculated using given equation (42) [20].

$$[Q_{RVE}] = \sum V_{ip}[Q_i]_p + V_{mp}[Q_m] \; i = w(warp), f(filler), z(binder) \quad (42)$$

Where, V_{ip} & m are the proportion of volume of any constituent tow sets and matrix between tows respectively.

The global stiffness matrix of representative volume element is determined by the inverse of the global compliance matrices as given, see equation (43) [20].

$$[S_{RVE}] = [Q_{RVE}]^{-1} \quad (43)$$

The engineering elastic constants (E_x, E_y, E_z, G_{yz}, G_{zx}, G_{xy}, ν_{xy}, ν_{yz}, ν_{xz}) of 3D orthogonal composite RVE are calculated with the help of global compliance matrix by given equations(44) [20].

$$E_x = \frac{1}{S_{11}}, \quad E_y = \frac{1}{S_{22}}, \quad E_z = \frac{1}{S_{33}}$$
$$\nu_{xy} = -\frac{S_{21}}{S_{11}}, \quad \nu_{xz} = -\frac{S_{31}}{S_{11}}, \quad \nu_{yz} = -\frac{S_{32}}{S_{22}} \quad (44)$$
(44)
$$G_{yz} = \frac{1}{S_{44}}, \quad G_{zx} = \frac{1}{S_{55}}, \quad G_{xy} = \frac{1}{S_{66}}$$

The following constitutive equation (46) characterizes the

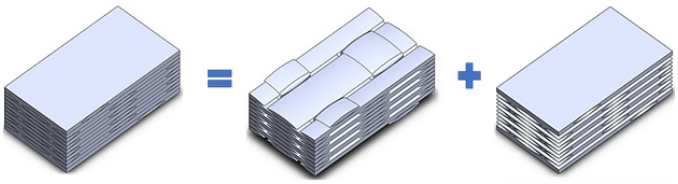

Figure 5: Lenticular Cross-sectional Model.

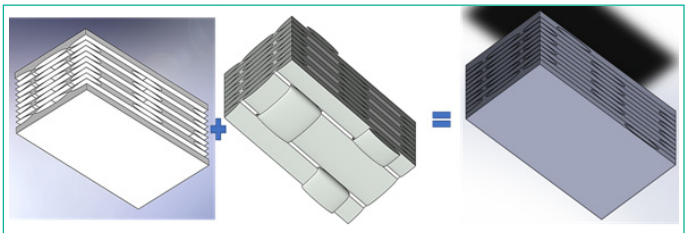

Figure 6: Elliptical Cross-sectional Model.

mechanical behavior of the composite:

$$\sigma = C.\varepsilon \quad (45)$$

Where σ = macro stress vector, ε = macro strain vector, C = macro-scale orthotropic elasticity matrix.

After developing a geometric model and a mechanical model as the first two steps in the process, the parameters of the materials have been entered, and the values of the stiffness and compliance matrices have been computed. In order to predict the stiffness matrix of 3D woven orthogonal composites, researchers have used both a geometrical model created by Buchanan et al. [19] and updated by B.P. Dash et al. [21] and a simplified analytical model developed by A. Mahmood et al. At the representative volume element level, this Model employs volume averaging and iso-strain homogeneous boundary conditions. In this model, the tow is a unidirectional lamina that is transversely isotropic. The elastic constants of transversely isotropic yarns relative to the local coordinate system can be determined using the Chamis micromechanics equations.

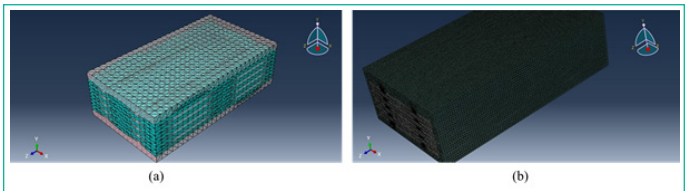

Figure 7: Mesh of unit Model (a) Lenticular, (b) Elliptical Models by Hypermesh.

Computational Modelling

The steps for the modelling and simulation of the composites are given as:

Step 1: The CAD model has been created using Solid works software to represent the 3D orthogonal woven structural unit cell with elliptical and lenticular cross-sections, as shown in Figures 5 and 6, respectively. The geometric parameters of yarn used in the model were determined based on 600 tex E-Glass fiber. However, it is important to note that while creating this model in Solid works, several assumptions have been made that may not reflect the real-world scenario. For instance, the yarns were assumed to have a uniform shape and size throughout the structure, and were assumed to be incompressible. Additionally, the yarns were assumed to be in a straight path and not have any crimp. However, in actual fabrics, filler yarns have undulations due to the binder crossing over them and holding them tightly bound. Furthermore, it should be noted that when modeling a composite, no voids or air bubbles were considered in the model. However, in reality, air bubbles or voids are present in the composite plate throughout the VARTM (Vacuum-Assisted Resin Transfer Molding) process. These voids or air bubbles can affect the mechanical properties of the composite and can lead to a reduction in strength and stiffness. Therefore, it is important to keep these factors in mind while using the CAD model to make any predictions about the behavior of the composite structure. It is recommended to use a more accurate and realistic model that takes into account all the above-mentioned factors to obtain more reliable results.

Step 2: In the second step the CAD model is imported into the Hyper mesh Software for meshing of model. Tetrahedron solid element has been choose for analysis due to complexity model and dependent type of mesh are created on both fabric and matrix of the Model, which is shown in Figure 7.

Although the modelling can be done in ANSYS and SOLIDWORKS, different software is required to mesh these models

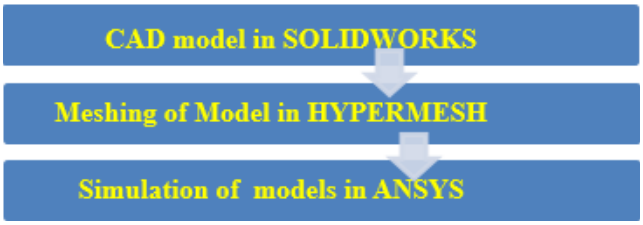

Figure 8: Flow chart of Numerical Modeling.

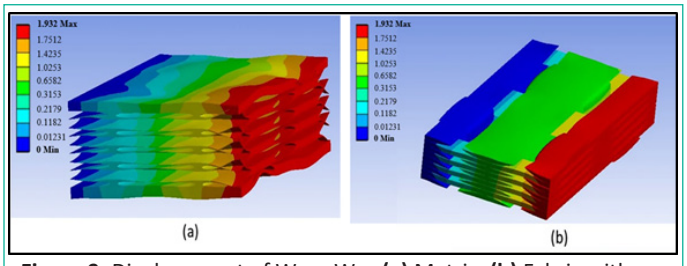

Figure 9: Displacement of Warp Way **(a)** Matrix, **(b)** Fabric with Lenticular Cross-section.

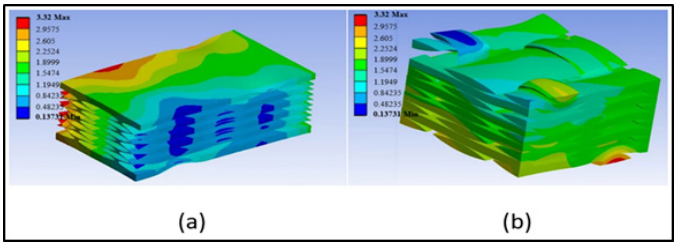

Figure 10: Displacement of Weft Way **(a)** Matrix, **(b)** Fabric with Lenticular Cross-section.

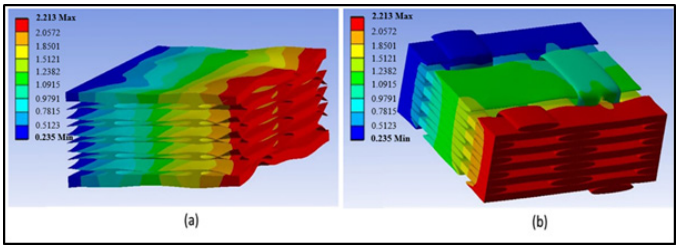

Figure 11: Displacement of Warp Way **(a)** Matrix, **(b)** Fabric with Elliptical Cross-section.

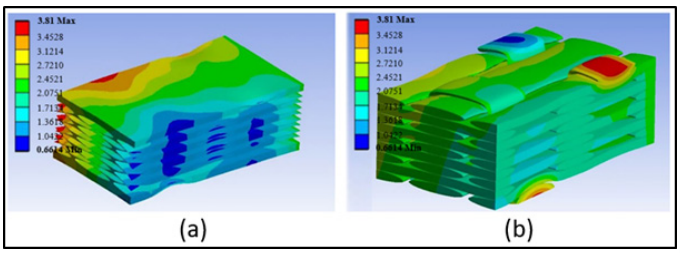

Figure 12: Displacement of Weft Way (a) Matrix, (b) Fabric with Elliptical Cross-section.

because meshing fails for element sizes below than 0.3 mm and thus the meshing does not work properly because the yarns have small dimensions and the elliptical binder is rotated at a 90° angle, so HYPERMESH software is used for meshing with 0.1 mm element size.

Step 3: In this step meshed file of model is imported into the FEA Software i.e., ANSYS, static structural module is used for analysis of model and the boundary conditions are same according to the experimental, boundary conditions are one end of the composite is fixed, separately in both warp and weft directions and then the opposite end is getting displaced with the displacement of 2mm/min then output is determined using ANSYS postprocessing process. The flow-chart for the computational modeling is shown in the Figure 8.

Results and Discussion

Computational Results

A Finite Element Method (FEM) was used for predicting the tensile property of 3D woven composite based on two yarn cross-sections. The CAD geometry of the woven composite is exported to a hyper mesh software to build a mesh in which a rectangular RVE is defined; it was used to predict the mechanical property of entire model. There are two procedures in FEA software (ANSYS): pre-processing and postprocessing. Adequate boundary conditions were applied, and fibre and matrix parameters were derived from the Ansys material data platform. During post-processing, the composite performance was examined under the displacement load. The displacement of the models for lenticular cross-section in warp direction are shown in figure 9 while in weft direction is shown in Figure 10. The displacement of the elliptical cross-sectional Model in warp and weft directions are shown in Figures 11 and 12 respectively.

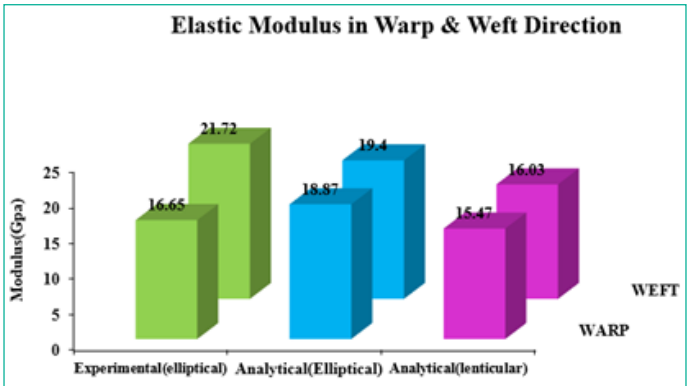

Figure 13: Comparison of Elastic Modulus in Warp and Weft Directions.

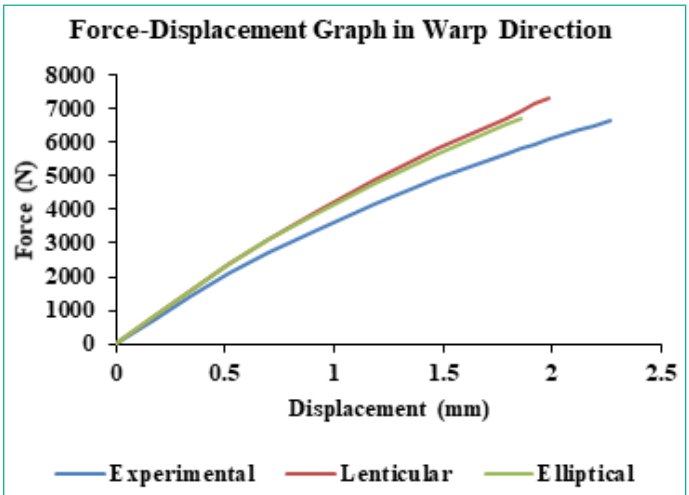

Figure 14: Force-Displacement Graph in Warp direction.

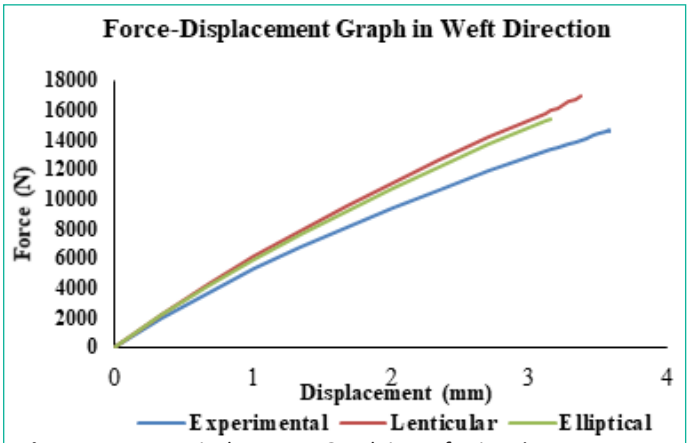

Figure 15: Force-Displacement Graph in Weft Direction.

It is observed that maximum displacement of weft direction is higher in both cases, i.e., elliptical and lenticular yarn.

Comparison between Experimental and Analytical Results

The results obtained from the analytical Models and experimental model are tabulated in table 3. Both the model's results exhibited a slight difference than the results obtained from the experimental results, but within the tolerance limit in the case of elliptical cross sections. The results given in table 3 can be shown in graphical form. The comparison between experimental and analytical results in warp and weft directions is shown in Figure 13.

Figure 13 shows that the elliptical cross-sectional model has a greater elastic modulus in both the warp and weft orientations than the lenticular cross-sectional model. This is because the elliptical cross-sectional Model has a lower thickness and thus a higher fibre volume fraction than the lenticular cross-sec-

tion. When compared to the lenticular cross-sectional model, a higher fibre volume percentage yields a higher modulus.

Comparison between Experimental and Computational Results

The comparison between experimental and computational results can be shown by the force vs displacement graphs. The force-displacement graph is shown in warp direction in Figure 14. There is some discrepancy between the estimated value and the experimental value. Errors of 13.26% in elliptical cross-sections and 15.80% in lenticular cross-sectional models have been calculated.

In Weft direction, the errors are calculated as 13.50% in elliptical cross-sectional model and 19.35% in lenticular cross-sectional model. This can be seen in Figure 15. The modulus of composite is larger in the weft direction than in the warp direction, as seen by the two graphs above. This is because the fibre volume percentage is greater in the weft direction than in the warp direction. The predicted values of modulus are higher than the measured values from the experimentation, as shown in the graphs, because in models, the undulations of the yarns are not considered, and the yarns are also assumed to have a specific shape, such as elliptical or lenticular throughout the fabric, which is not the case. Also, there are voids present in the real composite while during computational modelling, the composite is considered having no voids.

Conclusion

The tensile behaviour of a 3D orthogonal woven (4-stuffer layers) composite of two different yarn cross-sections (lenticular and elliptical) was predicted through computational modelling based on established analytical model. For computational modelling, unit cells of that woven structure were created on SOLIDWORKS software varying those two yarn cross-sections. The simulation for both the yarn cross-sections was performed in ANSYS software.

- The computational results of elliptical and lenticular cross-sections were compared with the experimentally achieved results for evaluating the congruency among them.

- The ellipsoidal and lenticular cross-sections of 3D woven preform were examined in this instance since they are the most prevalent cross-section among established models. Both the cross-sections have the same cross-sectional area as well as aspect ratio, it is 11.

- It has been observed that the elliptical cross-sectional Model gave good agreement with the experimentally gained values, while analysing the geometrical and mechanical features of that composite.

This study is aimed to save the time and experimental expenditure for researchers in predicting the micro-mechanical behaviour of 3D woven composite structures for their usage in various load-bearing application.

Author Statements

Declaration of Conflicting Interests

The author(s) declared no potential conflicts of interest with respect to the research, authorship, and/or publication of this article.

Funding

The author(s) received no financial support for the research, authorship, and/or publication of this article.

References

1. Behera BK, Jain M, Tripathi L, Chowdhury S. Low-velocity impact behaviour of textile-reinforced composite sandwich panels. Sandwich Compos. 2022; 213-260.
2. Tripathi L, Chowdhury S, Behera BK. Modeling and simulation of impact behavior of 3D woven solid structure for ballistic application. J Ind Text. 2022; 51: 6065-6086.
3. Nayak SY. Effect of CNT-based resin modification on the mechanical properties of polymer composites. Front Mater. 2021; 7: 609010.
4. Buchanan S, Grigorash A, Quinn JP, McIlhagger AT, Young C. Modelling the geometry of the repeat unit cell of three-dimensional weave architectures. J Text Inst. 2010; 101: 679-685.
5. Kamble Z, Mishra RK, Behera BK, Tichỳ M, Kolář V, Müller M. Design, development, and characterization of advanced textile structural hollow composites. Polymers. 2021; 13: 3535.
6. Kamble Z, Behera BK. A novel geometric model of four-directional 3D braided preforms. J Ind Text. 2022; 51: 1701-1715.
7. Tripathi L, Behera SK, Behera BK. Numerical modeling of flatwise energy absorption behavior of 3D woven honeycomb composites with different cell structures. J Sandw Struct Mater. 2022; 24: 2047-2064.
8. Dhiman S, Potluri P, Silva C. Influence of binder configuration on 3D woven composites. Compos Struct. 2015; 134: 862-868.
9. Mahmood A, Wang X, Zhou C. Generic stiffness model for 3D woven orthogonal hybrid composites. Aerosp Sci Technol. 2013; 31: 42-52.
10. Dash BP, Behera BK, Mishra R, Militky J. Modeling of internal geometry of 3D woven fabrics by computation method. J Text Inst. 2013; 104: 312-321.
11. Labanieh AR, Legrand X, Koncar V, Soulat D. Evaluation of the elastic behavior of multiaxis 3D-woven preforms by numerical approach. J Compos Mater. 2014; 48: 3243-3252.
12. Shah SZH, Yusoff PSM, Karuppanan S, Sajid Z. Elastic constants prediction of 3D fiber-reinforced composites using multiscale homogenization. Processes. 2020; 8: 722.
13. Mahmood A, Wang XW, Zhou CW. Generic geometric model for 3D woven interlock composites. Advanced Materials Research, Trans Tech Publ. 2012; 478–85.
14. Nehme S. Numerical/analytical methods to evaluate the mechanical behavior of interlock composites. J Compos Mater. 2011; 45: 1699-1716.
15. Dash BP, Behera KB. A study on structure property relationship of 3D woven composites. Mater Today Proc. 2015; 2: 2991-3007.
16. Behera BK, Dash BP. An experimental investigation into the mechanical behaviour of 3D woven fabrics for structural composites. Fibers Polym. 2014; 15: 1950-1955.
17. Cox BN, Dadkhah MS, Morris WL, Flintoff JG. Failure mechanisms of 3D woven composites in tension, compression, and bending. Acta Metall Mater. 1994; 42: 3967-3984.
18. Callus PJ, Mouritz AP, Bannister MK, Leong KH. Tensile properties and failure mechanisms of 3D woven GRP composites. Compos Part Appl Sci Manuf. 1999; 30: 1277-1287.

19. Buchanan S, Grigorash A, Quinn JP, McIlhagger AT, Young C. Modelling the geometry of the repeat unit cell of three-dimensional weave architectures. J Text Inst. 2010;101(7):679-685,.

20. Mahmood A, Wang X, Zhou C. Generic stiffness model for 3D woven orthogonal hybrid composites. Aerosp Sci Technol. 2013;31(1):42-52,.

21. Dash BP, Behera BK, Mishra R, Militky J. Modeling of internal geometry of 3D woven fabrics by computation method. J Text Inst. 2013 Mar;104(3):312-321,.

22. Mechanics of Composite Materials: Past, Present and Future - NASA Technical Reports Server (NTRS [Internet]. Available from: https://ntrs.nasa.gov/citations/19880008360